TrkBT1 Induces Liver Metastasis of Pancreatic Cancer Cells by Sequestering Rho GDP Dissociation Inhibitor and Promoting RhoA Activation

Zhongkui Li,[1] Zhe Chang,[1] Lucia J. Chiao,[4] Ya'an Kang,[1] Qianghua Xia,[1] Cihui Zhu,[1] Jason B. Fleming,[1] Douglas B. Evans,[5] and Paul J. Chiao[1,2,3]

Departments of [1]Surgical Oncology and [2]Molecular and Cellular Oncology, The University of Texas M.D. Anderson Cancer Center; [3]Program of Cancer Biology, The University of Texas Graduate School of Biomedical Sciences at Houston, Houston, Texas; [4]The University of Texas at Austin, Austin, Texas; and [5]Medical College of Wisconsin, Milwaukee, Wisconsin

Abstract

Many genetic and molecular alterations, such as *K-ras* mutation and NF-κB activation, have been identified in pancreatic cancer. However, the mechanisms by which pancreatic cancer metastasizes still remain to be determined. Although we previously showed that the tropomyosin-related kinase B (TrkB) was significantly correlated with the development of liver metastasis, its function in pancreatic cancer metastasis remained unresolved. In the present study, we showed that overexpressed TrkB is an alternatively spliced transcript variant of TrkB (TrkBT1) with a unique COOH-terminal 12–amino acid sequence and is mainly localized in the cytoplasm. Our results showed that overexpression of Flag-tagged TrkBT1 but not a Flag-tagged TrkBT1 COOH-terminal deletion mutant (Flag-TrkBT1ΔC) in nonmetastatic pancreatic cancer cells enhanced cell proliferation, promoted formation of colonies in soft agar, stimulated tumor cell invasion, and induced liver metastasis in an orthotopic xenograft mouse model of pancreatic cancer. TrkBT1 interacted with Rho GDP dissociation inhibitor (GDI) *in vivo*, but Flag-TrkBT1ΔC did not. Furthermore, overexpression of Flag-TrkBT1 and knockdown of RhoGDI expression by RhoGDI short hairpin RNAs promoted RhoA activation, but Flag-TrkBT1ΔC overexpression did not. Therefore, our results showed that TrkBT1 overexpression induces liver metastasis of pancreatic cancer and uncovered a unique signaling mechanism by which TrkBT1 sequesters GDI and activates RhoA signaling. [Cancer Res 2009;69(19):7851–9]

Introduction

Pancreatic adenocarcinoma is the fourth leading cause of adult cancer deaths in the United States (1). The 5-year survival rate ranges from 1% to 3%, and the median survival duration after diagnosis is <6 months (1). At the time of diagnosis, most patients with pancreatic cancer present with locally advanced or metastatic disease (2, 3). Because of these factors and the fact that it is characterized by a poor prognosis and lack of response to conventional therapy (3, 4), pancreatic cancer poses one of the greatest challenges in cancer research and treatment. Although many genetic and molecular alterations have been identified in pancreatic cancer based on the most frequently detected changes in patients with this disease (5), the underlying mechanisms by which pancreatic cancer cells become invasive and metastatic also remain to be elucidated.

Studies of liver metastases of human pancreatic cancer have been complicated by several difficulties. For example, no liver metastatic lesions can be obtained for analysis because surgery is not a treatment option for almost all patients with metastatic pancreatic cancer (6). Furthermore, few or no liver metastases samples can be spared from computed tomography–guided liver biopsy analysis. These issues have made obtaining samples of metastatic pancreatic cancer suitable for molecular analysis impossible through conventional methods, and a special program such as rapid autopsy of deceased pancreatic cancer patients is needed for collecting high-quality tissues from patients with metastatic pancreatic cancer (7, 8). To overcome this difficulty, Bruns and colleagues generated the highly liver metastatic Colo357L3.6pl pancreatic cancer cell line, a variant of the parental nonmetastatic Colo357FG pancreatic cancer cell line, using an orthotopic nude mouse model (9–12). To search for candidate genes overexpressed in pancreatic tumor invasion and metastasis, we previously performed a cDNA microarray analysis (9, 13) and showed that overexpression of tropomyosin-related kinase B (TrkB) was found in highly liver metastatic Colo357L3.6pl cells by cDNA microarray analysis and is correlated with perineural invasion, positive retroperitoneal margins, and early onset of liver metastasis of human pancreatic cancer (13), suggesting that TrkB overexpression may be involved in pancreatic cancer invasion and metastasis (13).

Neurotrophins and their receptors (p75NTR and the Trk family of receptors) play a plethora of roles in malignant cells. The *TrkB* gene is unusually large, spanning 355 kb (National Center for Biotechnology Information gene reference NC_000009.11). Because of alternative splicing and the use of different transcription termination (polyadenylation) sites, TrkB has multiple transcription variants and five major TrkB variants can be separated into three groups (Supplementary Fig. S1; ref. 14). TrkBT1 is a kinase domain absent TrkB variant with a unique COOH-terminal tail composed of 12 amino acids. Ohira and colleagues showed that TrkBT1 activated the RhoA signaling. However, the mechanisms by which TrkBT1 regulated RhoA activity have not been unequivocally shown (15).

In this report, we showed that overexpression of Flag-tagged TrkBT1 (Flag-TrkBT1), but not of a Flag-tagged TrkBT1 COOH-terminal deletion mutant (Flag-TrkBT1ΔC), in Colo357FG cells

induced colony formation in soft agar, cell invasion, and liver metastasis in an orthotopic xenograft mouse model of pancreatic cancer. We show that overexpressed TrkBT1 interacts with Rho GDP dissociation inhibitor (GDI) *in vivo*, thus uncovering a unique signaling mechanism by which TrkBT1 sequesters GDI and promotes RhoA activation.

Materials and Methods

Pancreatic tissue samples, cell lines, and cell culture. All of the human pancreatic cancer cell lines used in this study were grown in DMEM containing 10% fetal bovine serum and incubated at $37°C$ in a humidified atmosphere of 5% CO_2. Colo357FG and Colo357L3.6pl cells were described previously (9).

Mice. Female nude athymic BALB/c mice were purchased from Charles River Laboratories, Inc. Half million viable PANC-1, Colo357FG, Colo357L3.6pl, Colo357FG/Vec, Colo357FG/TrkBT1, Colo357FG/TrkBT1ΔC, Colo357FG/GDI-Sh1, PANC-1/Vec, and PANC-1/GDI-Sh1 cells, as determined by trypan blue exclusion assay, were suspended in 50 μL of PBS with 10% Matrigel and carefully injected into the pancreatic parenchyma of each mouse. There was no detectable leakage during tumor cell injection as described in a previous report (9). The animal protocol was approved by the M. D. Anderson Institutional Animal Care and Use Committee.

Reverse transcription-PCR. Reverse transcription (RT) reaction with oligo(dT) primers and PCR were performed as described previously (16).

Plasmid construction, transfection, and in vivo tumor imaging. pCMV-Tag4A-Flag-TrkBT1 (NM_001007097) and pCMV-Tag4A-Flag-TrkBT1ΔC plasmids, including pCMV-Tag4A empty vector for generation of control cells, were transfected into Colo357FG and PANC-1 cells using FuGENE 6 (Roche) according to the manufacturer's recommendations. A range of G418 concentration (100–1,000 μg/mL) was used to test the sensitivity to G418, and 500 μg/mL were used to select stably transfected Colo357FG/Vec, Colo357/TrkBT1, and Colo357/TrkBT1ΔC cells with untransfected Colo357FG cells as selection controls. Rho GDI1 short hairpin RNA (shRNA) lentiviral plasmids (pLKO.1-puro) were purchased from Sigma. Rho GDI1 shRNA lentivirus was harvested from HEK293 cells 48 h after transfection, as described by Tiscornia and colleagues (17). For *in vivo* imaging, an enhanced green fluorescent protein (GFP)/firefly luciferase (fLuc) double-expressing cassette was introduced into pancreatic cancer cells by lentiviral infection. The *in vivo* tumor growth was monitored in real time using an IVIS imaging system (Xenogen; ref. 18).

MTT assay. An MTT assay was performed in triplicate on 96-well plates as previously described (19). The data were expressed as the mean ± SE for three independent experiments.

Cell invasion assay. Invasion assay was performed as previously described using 24-well plates by using a Matrigel-coated invasion chamber (BD Biosciences) with an 8.0-μm pore size positron emission tomography membrane coated with a thin layer of GFR Matrigel Basement Membrane Matrix (19). A representative field of each experiment was photographed with 4× lens and 2.5× magnification.

Cell fractionation. Cell plasma membrane, cytosolic, and nuclear fractions were prepared using a Qproteome Cell Compartment kit (Qiagen) according to the manufacturer's protocol.

Anchorage-independent growth. Colony formation assay with 1.0×10^4 cells per well seeded in soft agar was performed as previously described (20). Colonies larger than 0.05 mm were automatically counted. Means and 95% confidence intervals of three independent experiments were performed in triplicate.

Western blot analysis. Histologically normal pancreatic tissue and pancreatic adenocarcinoma samples, obtained at the institution Pancreatic Tumor Tissue Bank, and cultured pancreatic cancer cells were used to obtain protein extracts. Western blot analysis was performed as previously described (21).

Coimmunoprecipitation. Protein extracts (1 mg) were subjected to immunoprecipitation with 1 μg of an anti-Flag M2 antibody (Sigma) linked with agarose beads at $4°C$ for 2 h. The immunoprecipitates were eluted with Flag peptide and subjected to Western blotting with anti-Rho GDI1 and anti-Flag M2-horseradish peroxidase (HRP) antibodies.

Immunocytochemistry. Immunostaining of TrkB was performed using an anti-TrkB antibody (BD Biosciences), and quantification of immunostainings was performed by averaging two sets of independently obtained results from five microscopic fields (22).

Rho activation assay. A standard assay comprised a pull-down assay using glutathione *S*-transferase (GST)–Rhotekin–Rho binding domain (RBD) protein beads and a monoclonal anti-RhoA antibody (Santa Cruz Biotechnology) according to the manufacturer's protocol.

Rho-associated kinase activity assay. Rho-associated kinase (ROCK) kinase activity was measured by ROCK activity immunoblot kit using a recombinant MYPT1 as substrate and anti–phospho-MYPT1 Thr^{696} according to the manufacturer's instruction (Cell Biolabs, Inc.).

Statistical analysis. All statistical analyses were performed with NCSS software. The significance of the data was determined by using the χ^2 test and Fisher's exact. A value of $P < 0.05$ was considered significant.

Results

TrkBT1 but not full-length TrkB is overexpressed in pancreatic cancer cells. We previously identified *TrkB* as an overexpressed gene in metastatic pancreatic cancer. Because of the existence of multiple transcription variants of TrkB and the functional diversity of different TrkB variants (Supplementary Fig. S1), we sought to further characterize the expression of individual variants of TrkB in pancreatic tumor samples and several pancreatic cancer cell lines. The results are shown in Fig. 1 and summarized in Supplementary Table S1. By analyzing TrkB expression using RT-PCR with variant-specific primers, we found that of the five major TrkB variants, only TrkBT1/variant b was detectable in highly liver metastatic Colo357L3.6pl cells (Fig. 1*A*). All the major TrkB variants were detectable in a glioma cell line, SNB19, as a RT-PCR–positive control to confirm the specificity and sensitivity for the optimized PCR conditions (Fig. 1*A*). Equal amounts of cDNA were indicated by glyceraldehyde-3-phosphate dehydrogenase (GAPDH) level (Fig. 1*A* and *B*). We also found overexpression of TrkBT1 in other metastatic pancreatic cancer cell lines Capan-2, BxPc-3, and Hs766T (Fig. 1*B, top*; refs. 23–25) and in seven pancreatic tumor samples but much lower expression levels in the nonmetastatic pancreatic tumor cell lines MiaPaCa-2, PANC-1, and MDAPanc-28 (Fig. 1*B, bottom*; refs. 19, 26, 27). TrkBT1 expression was undetectable in normal pancreatic tissue samples and immortalized human pancreatic ductal epithelial (HPDE) cells (Fig. 1*B*). Direct sequencing of PCR products confirmed that the amplified product of TrkBT1 is wild-type (data not shown).

To confirm the TrkBT1 overexpression in the pancreatic cancer cell lines and pancreatic tumor samples, we performed Western blot analysis to determine its protein expression level in these samples. The overexpressed TrkBT1 in Colo357L3.6pl cells has a molecular weight of ∼60 kDa, which is less than wild-type TrkB (145 kDa) and TrkBT1 (95 kDa) observed in SNB19 glioma cells (Fig. 1*C*; ref. 28). Sequencing of TrkBT1 cDNA cloned from Colo357L3.6pl cells verified the size of this full-length TrkBT1 protein, suggesting that 60-kDa TrkBT1 might lack posttranslational modifications. The results of this Western blotting confirmed that TrkBT1 was overexpressed in the highly metastatic cell lines, such as Colo357L3.6pl, BxPc-3, and Capan-2, but not in the nonmetastatic cell lines, such as Colo357FG, MiaPaCa-2, MDA-Panc-28, and PANC-1, suggesting that TrkBT1 overexpression is involved in pancreatic cancer invasion and metastasis (Fig. 1*D*).

TrkBT1 is primarily localized in the cytoplasm. To determine the function of overexpressed TrkBT1, we examined the localization of

TrkBT1 in Colo357L3.6pl cells by immunohistochemical analysis and cell fractionation. As shown in Fig. 2*A*, TrkBT1 was overexpressed in Colo357L3.6pl cells compared with Colo357FG. The overexpressed TrkBT1 was predominantly localized to the cytoplasm but not to the plasma membrane. We confirmed this finding using a cell fractionation assay with 30 μg of fractionated extracts enriched from membrane, cytosolic, and nuclear fractions of HEK293/Flag-TrkBT1, Colo357L3.6pl, and Colo357FG/Flag-TrkBT1. As shown in Fig. 2*B*, TrkBT1 protein, either endogenous (*right*) or ectopic (*left*), was strongly expressed in the cytosolic fraction but very weakly expressed in the membrane fraction and not expressed at all in the nuclear fraction. These results showed that overexpressed TrkBT1 is mainly localized in the cytoplasm and suggested that TrkBT1 signaling is independent of ligand brain-derived neurotrophic factor (BDNF) regulation and may have a novel signaling mechanism.

TrkBT1 overexpression stimulates cell growth. To further characterize TrkBT1 function in pancreatic cancer, we used RT-PCR to clone TrkBT1 and TrkBT1ΔC (deletion of the COOH-terminal 11 amino acids) into the mammalian expression vector pCMV-Tag4A to generate the COOH-terminal fusion Flag-Tag construct pCMV-Tag4A-TrkBT1 and pCMV-Tag4A-TrkBT1ΔC. The established constructs were sequenced to confirm no mutation in the cloned inserts, and both constructs were transfected into

nonmetastatic Colo357FG cells to produce stable expression clones using G418 selection. In addition, the empty vector pCMV-Tag4A was also transfected into Colo357FG to generate control cells, Colo357FG/Vec. We identified the overexpression of Flag-TrkBT1 and Flag-TrkBT1ΔC protein in G418-resistant clones using Western blotting with an anti-Flag M2 antibody. As shown in Supplementary Fig. S2*A* and *B*, we detected Flag-TrkBT1; compared the growth of Colo357FG/Vec, Colo357FG/TrkBT1, and Colo357FG/TrkBT1ΔC; and analyzed the growth of three Flag-TrkBT1–positive clones with different expression level at various time points using MTT assay. Our results indicated that the ectopic expression of TrkBT1ΔC had little effect to cell growth even at high expression level, whereas overexpression of TrkBT1 in Colo357FG cells significantly promoted cell growth (Supplementary Fig. S2*B*). These results suggest that cell growth was positively correlated to the expression level of TrkBT1 protein. Because TrkBT1 is overexpressed in metastatic pancreatic cancer, we selected the stable clone Colo357FG/TrkBT1c4 for additional experiments.

TrkBT1 up-regulates N-cadherin and vimentin expression and may contribute to epithelial-mesenchymal transition. As malignant progression of tumors is often associated with epithelial-mesenchymal transition (EMT), we examined the morphologic difference between Colo357FG/Vec and Colo357FG/TrkBT1. We also analyzed the expression of several EMT markers in
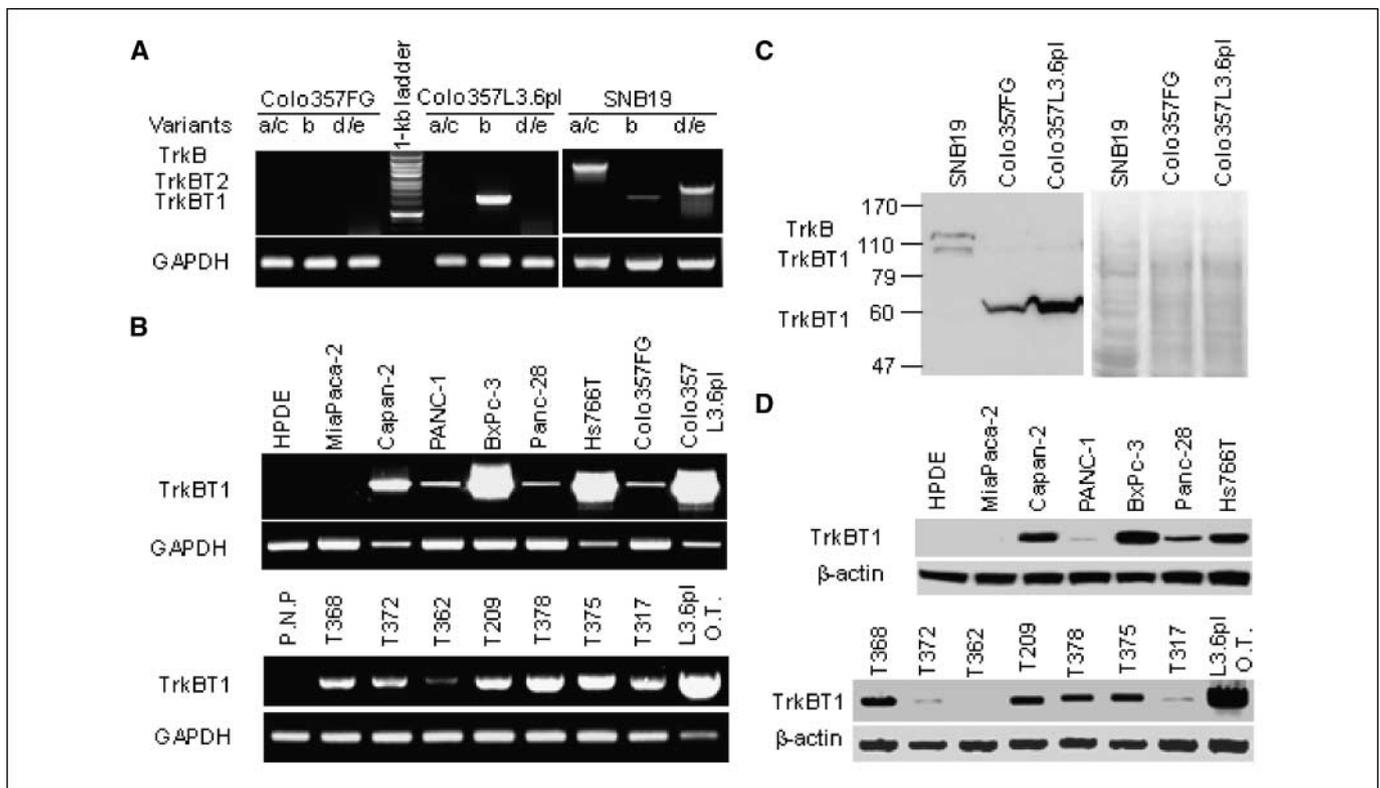
Figure 1. Expression of TrkBT1 in pancreatic cancer cell lines and pancreatic tumor tissue samples. *A,* analyzing the expression of TrkB variants by RT-PCR (30-cycle conditions) with variant-specific primers in Colo357FG and Colo357L3.6pl cells as indicated. Glioma cell line SNB19 was used as a positive control. *B,* RT-PCR analysis of TrkBT1 expression in the metastatic pancreatic cancer cell lines Capan-2, BxPc-3, Hs766T, and Colo357L3.6pl and in the nonmetastatic pancreatic cancer cell lines MiaPaCa-2, PANC-1, MDAPanc-28, and Colo357FG (40-cycle conditions) with TrkBT1/variant b–specific primers. Immortalized HPDE cells served as negative controls (*top*). Pancreatic tumors produced by Colo357L3.6pl (*L3.6pl O.T.*) cells orthotopically implanted in mice were used as a positive control. GAPDH was used as an internal cDNA loading control for both RT-PCR. *P.N.P.,* four pooled normal human adult pancreatic tissue samples (*bottom*). *C,* Western blot analysis of TrkB expression in Colo357FG and Colo357L3.6pl cells. The SNB19 glioma cell lysate was used as a positive control to indicate the posttranslational modification of full-length TrkB (145 kDa) and TrkBT1 (95 kDa). Staining of the Western blot membrane with Ponceau S was used to determine equal loading of the cell extracts. *D,* Western blot analysis of TrkBT1 protein expression in pancreatic cancer cell lines (*top*) and tumor tissue samples (*bottom*) as indicated. β-Actin was used as a loading control.

Colo357L3.6pl and Colo357FG cells with ectopic expression of Flag-TrkBT1 and TrkBT1ΔC using Western blot analysis. In Fig. 2C, Colo357FG/TrkBT1 shows motile and modest spindle cell morphology resembling mesenchymal cells. As shown in Fig. 2D,
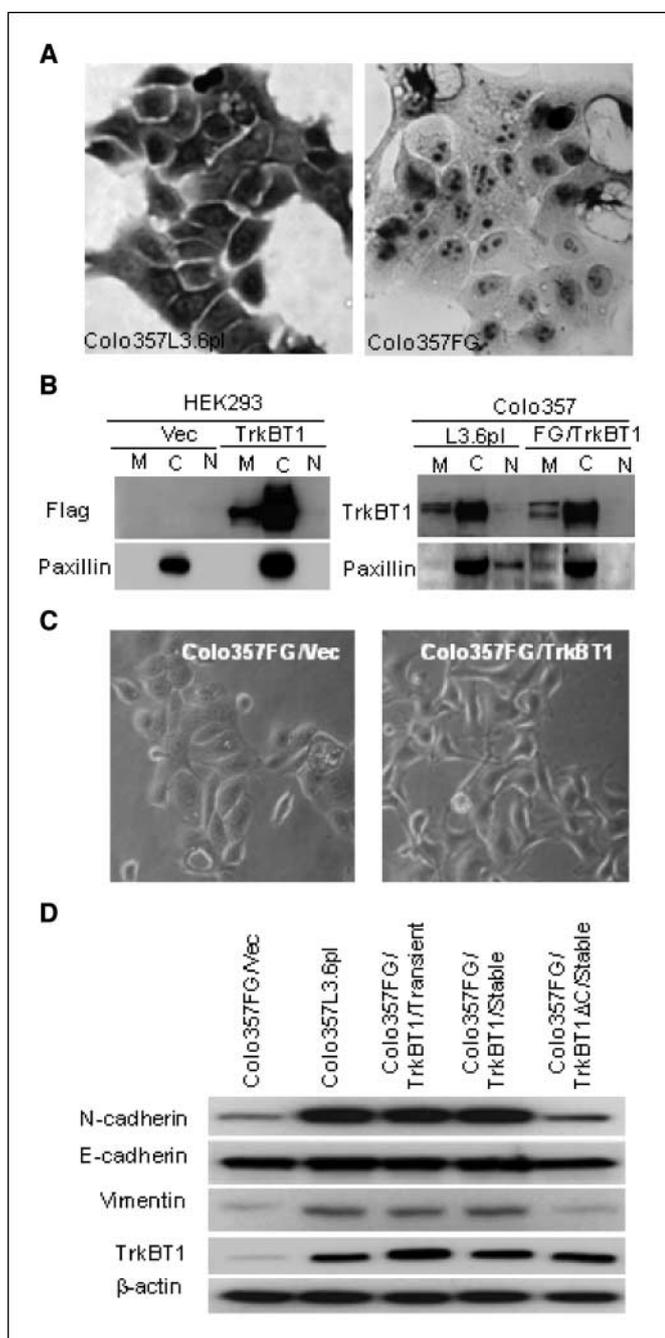

Figure 2. TrkBT1 cellular localization and its expression correlation with EMT markers. *A*, immunostaining showing the high expression and cytoplasmic localization of endogenous TrkBT1 in Colo357L3.6pl (*left*) compared with Colo357FG (*right*) cells. *B*, cell fractionation showing the cellular localization of the endogenous TrkBT1 in Colo357L3.6pl cells and the transfected Flag-TrkBT1 in HEK293 and Colo357FG cells as indicated. Paxillin was used as a cytosolic fraction marker. *M*, membrane; *C*, cytosolic; *N*, nuclear. *C*, morphology of Colo357FG (*left*) and Colo357FG/TrkBT1 (*right*) cells. *D*, Western blot analysis showing the expression of EMT markers (N-cadherin, E-cadherin, and vimentin) in TrkBT1-overexpressing Colo357L3.6pl cell line and Colo357FG expressing an empty vector, stably expressed TrkBT1, transiently transfected TrkBT1, and stably expressed TrkBT1ΔC.

expression of N-cadherin and vimentin was up-regulated in Colo357L3.6pl, Colo357FG/TrkBT1 (transient transfection), and Colo357FG/TrkBT1 cells (stable clones) but not in Colo357FG and Colo357FG/TrkBT1ΔC cells (stable clones). Expression of Flag-TrkBT1 did not alter the expression of E-cadherin in these tested pancreatic cancer cell lines (Fig. 2D). Because a key step in EMTs is the suppression of E-cadherin, these results suggested that overexpression of TrkBT1 may contribute to pancreatic tumor progression by inducing partial EMT as indicated by up-regulating the expression of some EMT markers, such as N-cadherin and vimentin.

TrkBT1 overexpression promotes anchorage-independent cell growth and tumor cell invasion *in vitro*. To test the anchorage-independent growth of TrkBT1-expressing cells, we examined the Flag-TrkBT1–stable clones described above using a colony formation assay in soft agar. Metastatic cell line Colo357L3.6pl was used as a positive control. As shown in Fig. 3A, overexpression of TrkBT1 but not TrkBT1ΔC in non-metastatic Colo357FG cells significantly enhanced the formation of colonies. In 0.8% soft agar, Flag-TrkBT1–expressing Colo357FG cells could form similar sizes and number of colonies as those observed in metastatic pancreatic cancer cell line Colo357L3.6pl. Flag-TrkBT1ΔC–expressing Colo357FG cells had no difference in colony formation compared with the control Colo357FG/Vec cells.

To determine whether TrkBT1 overexpression induced cell invasion *in vitro*, the Matrigel invasion assay was performed as described in Materials and Methods. The representative fields of cell invasion experiment are shown (Fig. 3B). These results showed that overexpression of TrkBT1 stimulated the invasion of Colo357FG and PANC-1 cells and the results from invasion assays were summarized in (Fig. 3B), suggesting that overexpression of TrkBT1 may play a role in pancreatic cancer metastasis by stimulating tumor cell invasion.

TrkBT1 overexpression and RhoGDI knockdown induce liver metastasis of pancreatic cancer in an orthotopic xenograft mouse model. Because the binding of RhoGDI1 to TrkBT1 may disrupt the interaction between RhoGDI1 and RhoA and lead to RhoA activation, we used the orthotopic xenograft mouse model to further determine whether ectopic expression of TrkBT1, or whether knocking down Rho GDI1, activates RhoA signaling and promotes liver metastasis (Supplementary Fig. S1B). To facilitate monitoring tumor growth *in vivo* using *in vivo* imaging system, lentiviral infection was used to introduce the GFP/fLuc dual expression cassette into the test cell lines Colo357FG/Vec, Colo357FG/TrkBT1, Colo357FG/TrkBT1ΔC, Colo357FG/GDI-Sh1, PANC-1/Vec, and PANC-1/GDI-Sh1. These GFP/fLuc-labeled stable transfectants were injected into the pancreases of nude mice. Although control cells (Colo357FG/Vec and PANC-1/Vec), TrkBT1-expressing cells (Colo357FG/TrkBT1), TrkBT1ΔC-expressing cells (Colo357FG/TrkBT1ΔC), and GDI shRNA–expressing cells (Colo357FG/GDI-Sh1 and PANC-1/GDI-Sh1) all formed large tumors, only Colo357FG/TrkBT1, Colo357FG/GDI-Sh1, and PANC-1/GDI-Sh1 cells had liver metastasis in nude mice in 8 weeks (Fig. 4; Supplementary Table S2). These results showed that expression of both TrkBT1 and GDI shRNA induced liver metastasis in Colo357FG and PANC-1 cells. Three Colo357FG pancreatic tumors and six Colo357FG/TrkBT1 liver metastatic lesions were collected for analysis of TrkBT1 expression by Western blot analysis. The representative experiments shown in Supplementary Fig. S3A confirmed the overexpression of TrkBT1 in the metastatic lesion of Colo357FG/TrkBT1 in all the samples. Taken together, these results
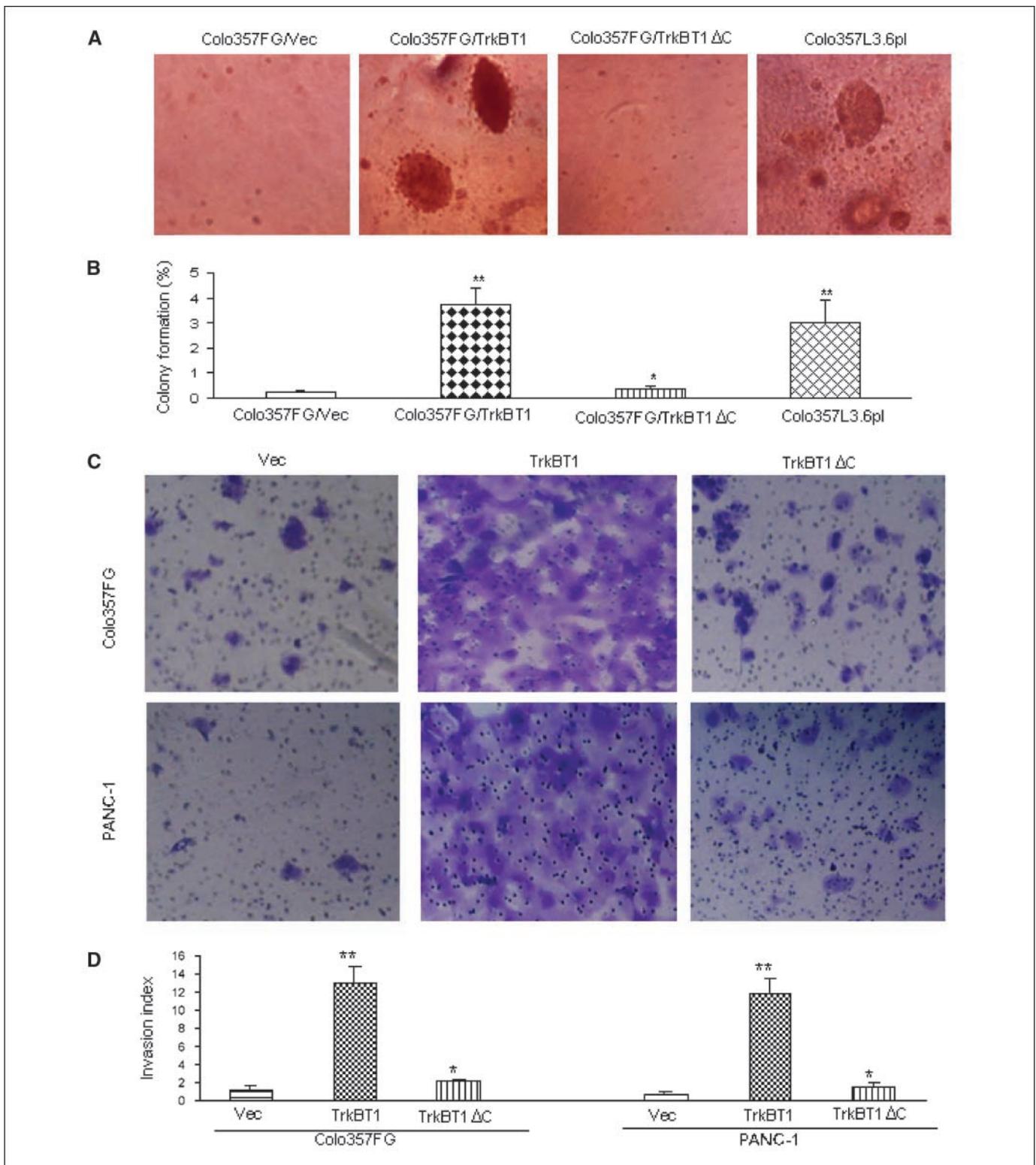
Figure 3. Stimulation of colony formation in soft agar and invasion in Matrigel-coated Boyden chamber by overexpression of TrkBT1. *A,* assay of colony formation in soft agar. Colo357L3.6pl, as a positive control, and Colo357FG-stable clones of vector control (*Vec*), TrkBT1, and TrkBT1ΔC were used to analyze the colony formation capacity as indicated. Representative images of Colo357L3.6pl, Colo357FG/Vec, Colo357FG/TrkBT1, and Colo357FG/TrkBT1ΔC clones. *B,* percentage of colony formation. The number of colonies was determined by counting duplicated plates. *Columns,* percentage of colony from the mean of three independent experiments with 10^4 input cells; *bars,* SE. *, $P > 0.05$; **, $P < 0.05$. *C,* cell invasion assay using Matrigel-coated Boyden chamber. Colo357FG/Vec, Colo357FG/TrkBT1, Colo357FG/TrkBT1ΔC, PANC-1/Vec, PANC-1/TrkBT1, and PANC-1/TrkBT1ΔC cells were added to the top compartment of a Matrigel-coated Boyden chamber. After incubation for 48 h, the noninvading cells were removed from the upper surface of the membrane. The invading cells were stained, photographed, and counted. The representative fields are shown. Magnification, ×10. *D,* invasion index. The number of cells that traversed Matrigel-covered filters was determined by counting duplicated inserts. *Columns,* mean of three independent experiments; *bars,* SE. *, $P > 0.05$; **, $P < 0.05$. NIH3T3 was used as control cells to calculate the cell invasion index according to the instructions for using Matrigel-coated invasion chamber by BD Biosciences.
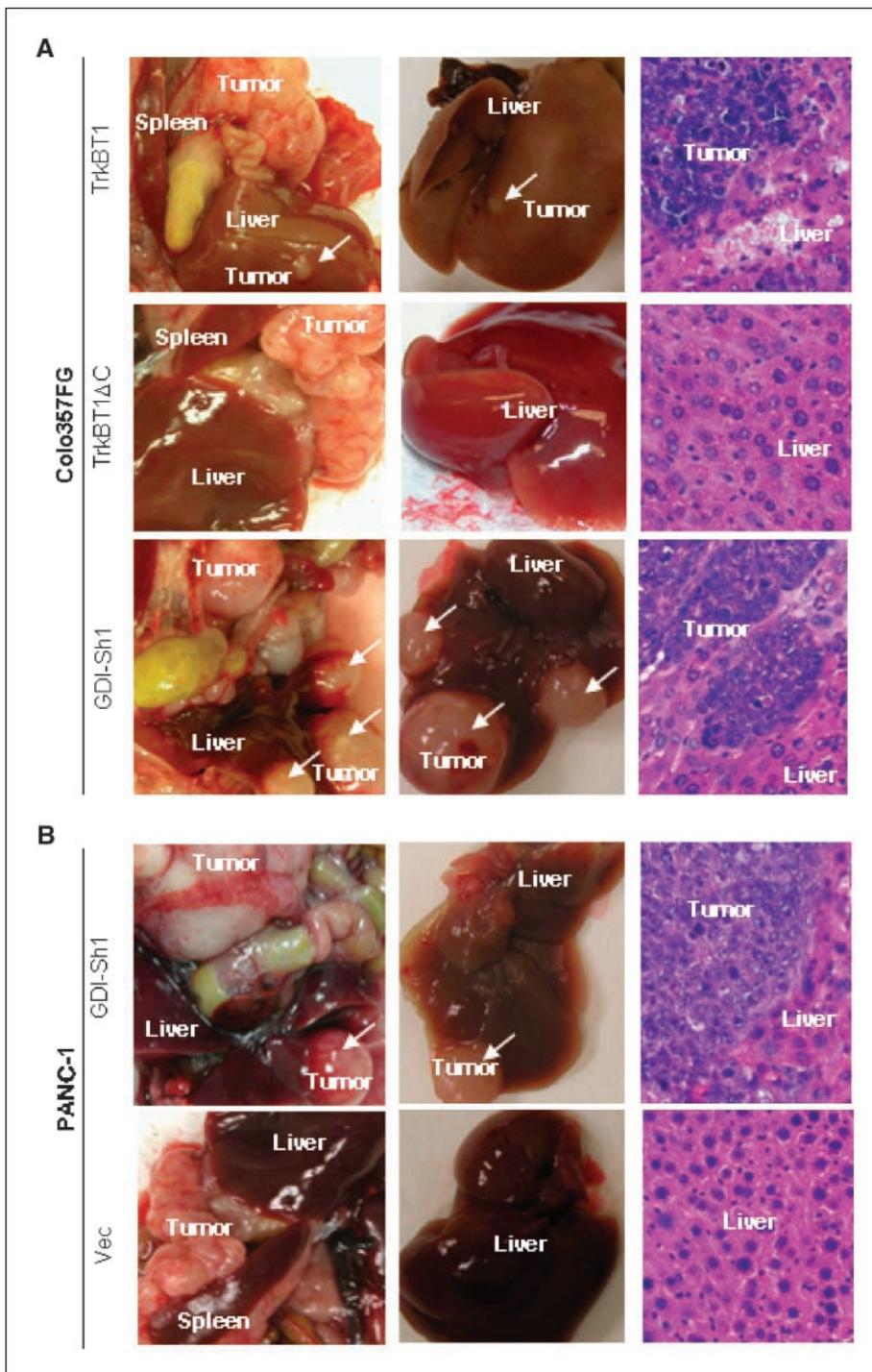
Figure 4. Pancreas-to-liver metastasis in orthotopic xenograft mouse model of pancreatic cancer. GFP/fLuc dual-labeled stable cell lines Colo357FG/Vec, Colo357FG/TrkBT1, Colo357FG/TrkBT1ΔC, Colo357FG/GDI-Sh1, PANC-1/Vec, and PANC-1/GDI-Sh1 were injected into the pancreases of mice to test their liver metastasis capacity. Representative images of dissected pancreas with tumor and liver with metastatic lesions. H&E staining of liver sections from each group. *A,* Colo357FG/TrkBT1, Colo357FG/TrkBT1ΔC, and Colo357FG/GDI-Sh1. *B,* PANC-1/Vec and PANC-1/GDI-Sh1.

suggest that overexpression of TrkBT1 plays a key role in the malignant progression of pancreatic cancer and a potential mechanism by which TrkBT1 may bind to Rho GDI1 through COOH-terminal tail of TrkBT1, which in turn reduces the inhibitory effect on RhoA and activates RhoA signaling.

The unique COOH-terminal tail of TrkBT1 is essential for promoting RhoA activation by sequestering GDI. As a result of alternative splicing, TrkBT1 has a unique COOH-terminal tail composed of 12 amino acids (GFVLFHKIPLDG). Overexpression of TrkBT1ΔC in Colo357FG cells induced neither the formation of

colonies in soft agar culture nor liver metastasis in orthotopic xenograft mouse model, suggesting that this unique COOH-terminal tail is a functional domain responsible for TrkBT1-induced phenotypic changes (Figs. 2–4).

To determine how the unique COOH-terminal tail affects cell signaling networks in promoting metastasis of pancreatic cancer, we examined the interaction between TrkBT1 and Rho GDI1 in pancreatic cancer cells. TrkBT1 physically interacted with Rho GDI1, and this interaction depended completely on the TrkBT1-specific COOH-terminal tail, as Flag-TrkBT1ΔC failed to bring

down Rho GDI1 in Colo357FG/TrkBT1ΔC cells (Fig. 5A, left). In addition, TrkBT1 overexpression had no effect on RhoA protein expression as indicated by Western blotting (Fig. 5A, right). These results suggested that the overexpressed TrkBT1 may sequester Rho GDI1 to facilitate Rho activation because Rho GDI1 is a negative regulator of RhoA activation. So, we further tested Rho

activation using GST-Rhotekin-RBD beads. Rhotekin is a scaffold protein and effector of RhoA. The RBD of Rhotekin specifically interacts with the active (GTP bound) form of RhoA, thus acting as an affinity reagent for monitoring RhoA activation. As indicated in a pull-down assay using Colo357L3.6pl cells (Fig. 5B, top, left), loading GTPγS (positive control) into cell lysates enhanced the

Figure 5. TrkBT1 interacts with Rho GDI1 and stimulates RhoA activation. *A*, identification of Rho GDI1 as a TrkBT1-interacting protein. *Left*, Colo357FG cells transfected with Flag-TrkBT1 or Flag-TrkBT1ΔC were subjected to immunoprecipitation with anti-Flag M2 antibody and to immunoblotting with anti-Flag M2-HRP and anti-RhoGDI1 antibodies. *Right*, Western blot analysis was performed to determine the levels of TrkBT1 and RhoA expression in Colo357FG, Colo357L3.6pl, Colo357FG/Flag-TrkBT1, and Colo357/Flag-TrkBT1ΔC. β-actin was used as a loading control. *B, top left*, binding assay with GST-Rhotekin-RBD protein beads for RhoA activation (loading GTPγS) and inactivation (loading GDP) using Colo357L3.6pl cell lysates; *top right*, determination of RhoA activation in cell extracts isolated from Colo357FG, Colo357L3.6pl, Colo357FG/Flag-TrkBT1, or Colo357FG/Flag-TrkBT1ΔC cells using GST-Rhotekin-RBD protein beads. *Bottom left*, immunoblot was performed to determine the expression levels of Flag-tagged TrkBT1, Flag-tagged TrkBT1ΔC, and RhoA in PANC-1/TrkBT1 and PANC-1/TrkBT1ΔC cells. Coomassie blue staining was used as a loading control; *bottom right*, determination of RhoA activation in cell extracts isolated from PANC-1/Vec, PANC-1/TrkBT1, and PANC-1/TrkBT1ΔC clones using GST-Rhotekin-RBD beads as described in Materials and Methods. *C*, Western blot analysis showing that three lentiviral Rho GDI1 shRNAs effectively down-regulated Rho GDI1 protein expression in Colo357FG (top, left) and PANC-1 (bottom, left) cells, and induction of RhoA activation in Colo357FG and PANC-1 cells with knockdown of Rho GDI1 expression (right). *D*, ROCK kinase activity was determined by phosphorylation of ROCK substrate, MYPT1. Recombinant ROCK1 was used as a positive control in lane 1.
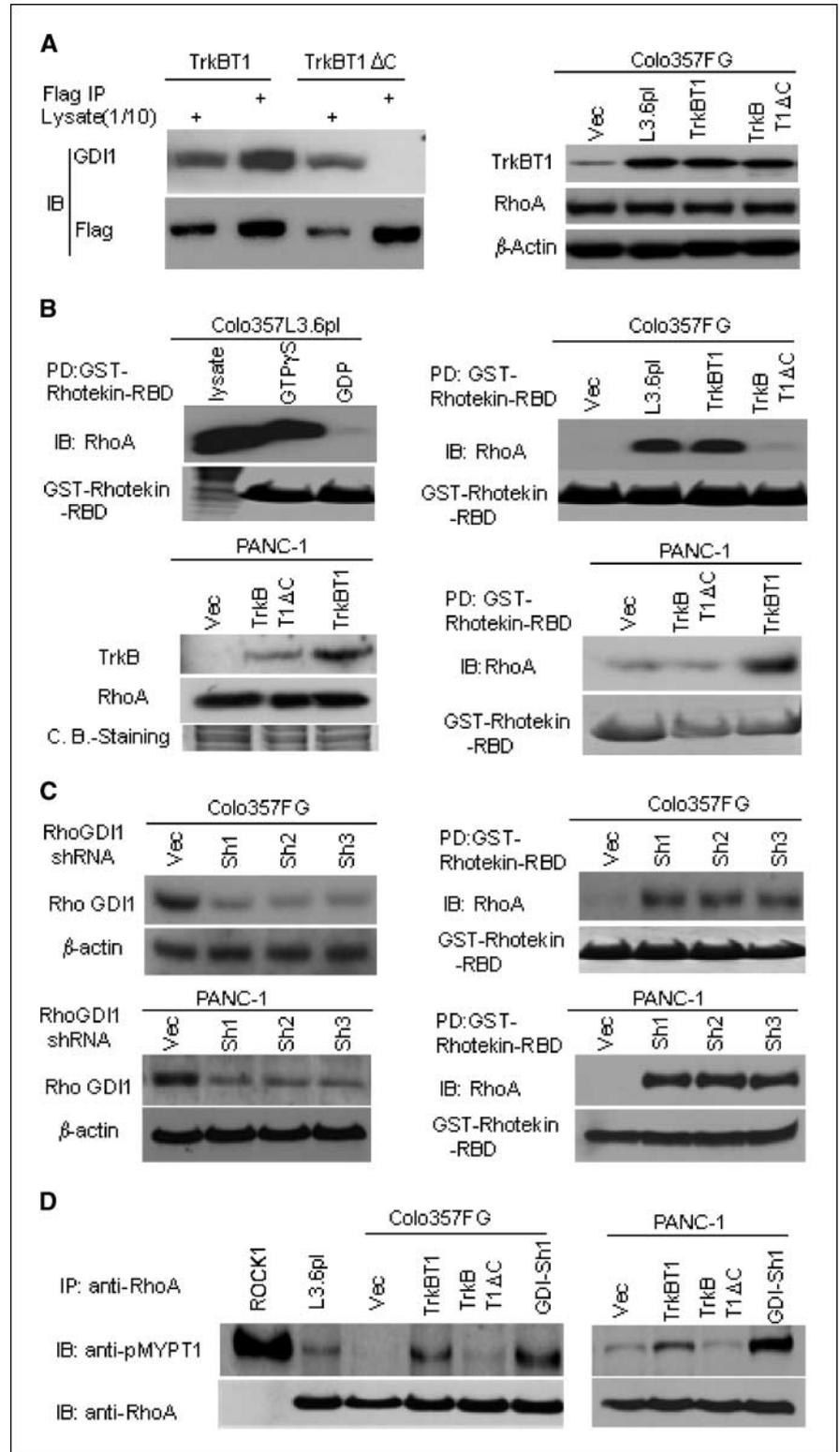
interaction between GST-Rhotekin-RBD and RhoA, whereas loading GDP (negative control) into the lysates significantly decreased this interaction, confirming that the GST-Rhotekin-RBD beads can detect activated RhoA. Thus, we performed a GST-Rhotekin-RBD binding assay using the cell extracts from Colo357L3.6pl, Colo357FG/Vec, Colo357FG/TrkBT1, and Colo357FG/TrkBT1ΔC cells. As shown in Fig. 5*B* (*top, right*), RhoA was constitutively activated in Colo357L3.6pl cells, but RhoA activation was not detectable in Colo357FG and Colo357FG/TrkBT1ΔC. To confirm RhoA activation by TrkBT1, we generated PANC-1/Flag-TrkBT1–stable, PANC-1/Flag-TrkBT1ΔC–stable, and PANC-1/Vec–stable cell lines. We determined the expression of Flag-TrkBT1, Flag-TrkBT1ΔC, and RhoA by Western blot (Fig. 5*B*, *bottom, left*). As shown in GST-Rhotekin-RBD binding assay using the cell extracts from these three cell lines, the expression of TrkBT1 but not TrkBT1ΔC stimulated RhoA activation in PANC-1 cells (Fig. 5*B*, *bottom, right*). These results showed that TrkBT1 overexpression induces activation of RhoA by sequestering RhoGDI1.

We reasoned that if TrkBT1 overexpression results in RhoA activation through sequestering Rho GDI1, then down-regulation of Rho GDI1 expression will have a similar effect and RhoA will be activated in cells with knockdown of Rho GDI1 expression. Therefore, to verify the findings on RhoA activation through TrkBT1-mediated sequestering Rho GDI1, we knocked down the Rho GDI1 expression in Colo357FG and PANC-1 cells using shRNAs via lentivirus-mediated infection. Three Rho GDI1 shRNAs effectively down-regulated the expression of Rho GDI1 protein (Fig. 5*C*, *left*) and stimulated RhoA activation (Fig. 5*C*, *right*). To further show the regulation of RhoA activity by TrkBT1 over-expression, we performed additional assays using MiaPaCa-2 (no TrkBT1 expression) and additional three pancreatic cancer cell lines with TrkBT1 overexpression, including BxPc-3, Capan-2, and Hs766T (Supplementary Fig. S3*C*). These results further suggest that TrkBT1 overexpression promotes RhoA activation. Moreover, TrkBT1 overexpression and Rho GDI shRNA–mediated down-regulation of Rho GDI1 expression in Colo357FG and PANC-1 cells resulted in activation of RhoA downstream major effector ROCK (Fig. 5*D*). These results suggested that TrkBT1 induces pancreatic cancer metastasis through induction of constitutive RhoA activation by sequestering Rho GDI1. Figure 6 sketches out our proposed working model for the mechanism RhoA activation by TrkBT1 overexpression, and the diagram shows that overexpressed TrkBT1 sequesters Rho GDI and relieves the inhibitory effect of RhoGDI on RhoA, which in turn promotes the RhoA activation through formation of GTP-bound RhoA. GTP-bound RhoA then activates its downstream effector ROCK. Consequently, ROCK signaling pathways may activate to regulate numerous cellular processes, including gene transcription, proliferation, adhesion, and migration.

Discussion

In this report, we identified that TrkBT1 was overexpressed in pancreatic tumor and several pancreatic cancer cell lines and that expression of TrkBT1, but not TrkBT1ΔC, in nonmetastatic cells enhances pancreatic tumor growth and colony formation, induces EMT, and promotes liver metastasis of pancreatic cancer in an established orthotopic mouse model. As summarized in Fig. 6, most interestingly, we found that overexpressed TrkBT1 stimulated Rho activation by sequestering GDI. Thus, we uncovered a novel signaling mechanism by which TrkBT1 overexpression–mediated
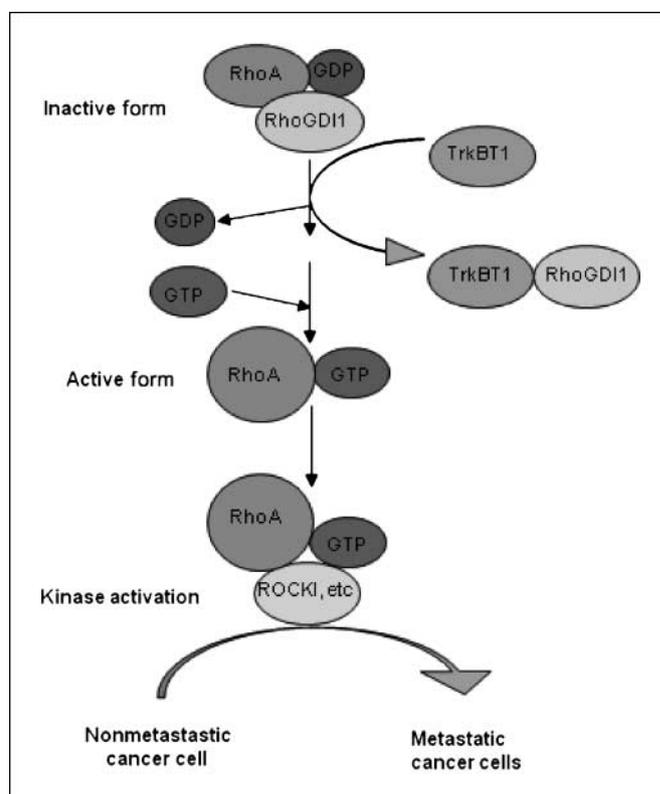
Figure 6. Working model for TrkBT1 signaling. The model suggests that TrkBT1-mediated sequester of Rho GDI may account for the activation of RhoA.

RhoA activation contributes to the development of liver metastasis of pancreatic cancer.

Our studies of TrkBT1 in pancreatic cancer cells showed that the unique COOH-terminal sequence of TrkBT1 binds to RhoGDI1, eliciting a unique type of signal transduction other than the well-understood regulation of the tyrosine kinase pathway (29). Ohira and colleagues (30) showed that TrkBT1 bound to Rho GDI1 in glial cells. The binding of BDNF to TrkBT1 caused Rho GDI1 to dissociate from the COOH-terminal tail of TrkBT1, resulting in morphologic changes in astrocytes (15). Consistent with this observation, our results showed that TrkBT1 interacted with RhoGDI1 to enhance RhoA activation in metastatic Colo357L3.6pl cells. However, this interaction may be independent of ligand BDNF regulation because TrkBT1 protein in Colo357L3.6pl cells is expressed primarily in the cytosol and not on the cell surface membrane (Fig. 2*C*).

Studies have shown that Rho GTPases play a role in invasion and metastasis of pancreatic cancer (31), colorectal cancer (32), bladder cancer (33), esophageal squamous cell carcinoma (34), and breast tumor (35). Kusama and colleagues (31) showed that p190 RhoGAP reduced human pancreatic cancer cell invasion and metastasis by inactivation of Rho GTPases. In addition, Kamai and colleagues (33) reported that RhoA activation was associated with invasion and lymph node metastasis of upper urinary tract cancer. In a study of colorectal cancer, Takami and colleagues (32) found that the level of expression of active RhoA protein in primary tumors correlated with lymph node metastasis. A recent study showed that overexpression of miR-31 suppressed metastasis of breast tumor cells and RhoA overexpression partially reverses miR-31–suppressed metastasis, further suggesting RhoA function in induction of metastasis (35). The active form of RhoA protein is

significantly higher in Colo357L3.6pl cells than in Colo357FG cells; however, the level of expression of RhoA protein in Colo357FG and highly metastatic Colo357L3.6pl cells does not differ (Fig. 5*B* and *C*). Most importantly, overexpression of TrkBT1 in Colo357FG and PANC-1 cells significantly stimulates activation of RhoA and liver metastasis of pancreatic cancer, whereas the COOH-terminal tail-deleted TrkBT1ΔC does not affect activation of RhoA. These results indicate that activation of RhoA (possibly including other Rho GTPases) is induced by the COOH-terminal tail of TrkBT1-mediated sequester of RhoGDI, which may account for the TrkBT1 overexpression–mediated capability of pancreatic cancer to metastasize to the liver.

Disclosure of Potential Conflicts of Interest

No potential conflicts of interest were disclosed.

Acknowledgments

References

1. Jemal A, Siegel R, Ward E, et al. Cancer statistics, 2008. CA Cancer J Clin 2008;58:71–96.
2. Crane CH, Varadhachary G, Pisters PW, Evans DB, Wolff RA. Future chemoradiation strategies in pancreatic cancer. Semin Oncol 2007;34:335–46.
3. Tamm EP, Loyer EM, Faria SC, Evans DB, Wolff RA, Charnsangavej C. Retrospective analysis of dual-phase MDCT and follow-up EUS/EUS-FNA in the diagnosis of pancreatic cancer. Abdom Imaging 2007;32:660–7.
4. Stathopoulos GP, Androulakis N, Souglakos J, Stathopoulos J, Georgoulias V. Present treatment and future expectations in advanced pancreatic cancer. Anticancer Res 2008;28:1303–8.
5. Hruban RH, Iacobuzio-Donahue C, Wilentz RE, Goggins M, Kern SE. Molecular pathology of pancreatic cancer. Cancer J 2001;7:251–8.
6. Evans DB, Lee JE, Pisters PW, et al. Advances in the diagnosis and treatment of adenocarcinoma of the pancreas. Cancer Treat Res 1997;90:109–25.
7. Iacobuzio-Donahue CA, Fu B, Yachida S, et al. DPC4 gene status of the primary carcinoma correlates with patterns of failure in patients with pancreatic cancer. J Clin Oncol 2009;27:1806–13.
8. Embuscado EE, Laheru D, Ricci F, et al. Immortalizing the complexity of cancer metastasis: genetic features of lethal metastatic pancreatic cancer obtained from rapid autopsy. Cancer Biol Ther 2005;4:548–54.
9. Bruns CJ, Harbison MT, Kuniyasu H, Eue I, Fidler IJ. *In vivo* selection and characterization of metastatic variants from human pancreatic adenocarcinoma by using orthotopic implantation in nude mice. Neoplasia 1999;1:50–62.
10. Vezeridis MP, Meitner PA, Tibbetts LM, Doremus CM, Tzanakakis G, Calabresi P. Heterogeneity of potential for hematogenous metastasis in a human pancreatic carcinoma. J Surg Res 1990;48:51–5.
11. Vezeridis MP, Tzanakakis GN, Meitner PA, Doremus CM, Tibbetts LM, Calabresi P. *In vivo* selection of a highly metastatic cell line from a human pancreatic carcinoma in the nude mouse. Cancer 1992;69:2060–3.
12. Sipos B, Moser S, Kalthoff H, Torok V, Lohr M, Kloppel G. A comprehensive characterization of pancreatic ductal carcinoma cell lines: towards the establishment of an *in vitro* research platform. Virchows Arch 2003;442:444–52.
13. Sclabas GM, Fujioka S, Schmidt C, et al. Overexpression of tropomysin-related kinase B in metastatic human pancreatic cancer cells. Clin Cancer Res 2005;11:440–9.
14. Stoilov P, Castren E, Stamm S. Analysis of the human TrkB gene genomic organization reveals novel TrkB isoforms, unusual gene length, and splicing mechanism. Biochem Biophys Res Commun 2002;290:1054–65.
15. Ohira K, Homma KJ, Hirai H, Nakamura S, Hayashi M. TrkB-T1 regulates the RhoA signaling and actin cytoskeleton in glioma cells. Biochem Biophys Res Commun 2006;342:867–74.
16. Li Z, Sclabas GM, Peng B, et al. Overexpression of synuclein-γ in pancreatic adenocarcinoma. Cancer 2004; 101:58–65.
17. Tiscornia G, Singer O, Verma IM. Production and purification of lentiviral vectors. Nat Protoc 2006;1:241–5.
18. Xie X, Xia W, Li Z, et al. Targeted expression of BikDD eradicates pancreatic tumors in noninvasive imaging models. Cancer Cell 2007;12:52–65.
19. Niu J, Li Z, Peng B, Chiao PJ. Identification of an autoregulatory feedback pathway involving interleukin-1α in induction of constitutive NF-κB activation in pancreatic cancer cells. J Biol Chem 2004;279:16452–62.
20. Melisi D, Ishiyama S, Sclabas GM, et al. LY2109761, a novel transforming growth factor β receptor type I and type II dual inhibitor, as a therapeutic approach to suppressing pancreatic cancer metastasis. Mol Cancer Ther 2008;7:829–40.
21. Fujioka S, Schmidt C, Sclabas GM, et al. Stabilization of p53 is a novel mechanism for proapoptotic function of NF-κB. J Biol Chem 2004;279:27549–59.
22. Wulfing P, Kersting C, Tio J, et al. Endothelin-1-, endothelin-A-, and endothelin-B-receptor expression is correlated with vascular endothelial growth factor expression and angiogenesis in breast cancer. Clin Cancer Res 2004;10:2393–400.
23. Marchesi F, Monti P, Leone BE, et al. Increased survival, proliferation, and migration in metastatic human pancreatic tumor cells expressing functional CXCR4. Cancer Res 2004;64:8420–7.
24. Uchima Y, Sawada T, Nishihara T, Maeda K, Ohira M, Hirakawa K. Inhibition and mechanism of action of a protease inhibitor in human pancreatic cancer cells. Pancreas 2004;29:123–31.
25. Lalani a S, Alters SE, Wong A, Albertella MR, Cleland JL, Henner WD. Selective tumor targeting by the hypoxia-activated prodrug AQ4N blocks tumor growth and metastasis in preclinical models of pancreatic cancer. Clin Cancer Res 2007;13:2216–25.
26. Fujioka S, Sclabas GM, Schmidt C, et al. Inhibition of constitutive NF-κB activity by IκBαM suppresses tumorigenesis. Oncogene 2003;22:1365–70.
27. Tsutsumi S, Yanagawa T, Shimura T, Kuwano H, Raz A. Autocrine motility factor signaling enhances pancreatic cancer metastasis. Clin Cancer Res 2004;10:7775–84.
28. Hamel W, Westphal M, Szonyi E, Escandon E, Nikolics K. Neurotrophin gene expression by cell lines derived from human gliomas. J Neurosci Res 1993;34:147–57.
29. Kryl D, Barker PA. TTIP is a novel protein that interacts with the truncated T1 TrkB neurotrophin receptor. Biochem Biophys Res Commun 2000;279:925–30.
30. Ohira K, Kumanogoh H, Sahara Y, et al. A truncated tropomyosin-related kinase B receptor, T1, regulates glial cell morphology via Rho GDP dissociation inhibitor 1. J Neurosci 2005;25:1343–53.
31. Kusama T, Mukai M, Endo H, et al. Inactivation of Rho GTPases by p190 RhoGAP reduces human pancreatic cancer cell invasion and metastasis. Cancer Sci 2006;97:848–53.
32. Takami Y, Higashi M, Kumagai S, et al. The activity of RhoA is correlated with lymph node metastasis in human colorectal cancer. Dig Dis Sci 2008;53:467–73.
33. Kamai T, Kawakami S, Koga F, et al. RhoA is associated with invasion and lymph node metastasis in upper urinary tract cancer. BJU Int 2003;91:234–8.
34. Faried A, Nakajima M, Sohda M, Miyazaki T, Kato H, Kuwano H. Correlation between RhoA overexpression and tumour progression in esophageal squamous cell carcinoma. Eur J Surg Oncol 2005;31:410–4.
35. Valastyan S, Reinhardt F, Benaich N, et al. A pleiotropically acting microRNA, miR-31, inhibits breast cancer metastasis. Cell 2009;137:1032–46.